THE JOURNAL OF BIOLOGICAL CHEMISTRY
Vol. 280, No. 13, Issue of April 1, pp. 12567–12572, 2005
Printed in U.S.A.

Steric Accessibility of the HIV-1 gp41 N-trimer Region*

Received for publication, November 11, 2004, and in revised form, January 4, 2005
Published, JBC Papers in Press, January 18, 2005, DOI 10.1074/jbc.M412770200

Agnes E. Hamburger‡§¶, Sunghwan Kim§‖, Brett D. Welch§‖, and Michael S. Kay‖****

From the ‖Department of Biochemistry, University of Utah School of Medicine, Salt Lake City, Utah, 84132 and the ‡Department of Biology, Massachusetts Institute of Technology, Cambridge, Massachusetts 02139

During human immunodeficiency virus entry, gp41 undergoes a series of conformational changes that induce membrane fusion. Immediately prior to fusion, gp41 exists in a prehairpin intermediate in which the N- and C-peptide regions of gp41 are exposed. Rearrangement of this intermediate into a six-helix bundle composed of a trimeric coiled coil from the N-peptide region (N-trimer) surrounded by three peptides from the C-peptide region provides the driving force for membrane fusion, whereas prevention of six-helix bundle formation inhibits viral entry. Because of its central role in mediating viral entry, the N-trimer region of gp41 is a key vaccine target. Extensive efforts to discover potent and broadly neutralizing antibodies (Abs) against the N-trimer region have, thus far, been unsuccessful. In this study, we attached a potent C-peptide inhibitor that binds to the N-trimer region to cargo proteins of various sizes to examine the steric accessibility of the N-trimer during fusion. These inhibitors show a progressive loss of potency with increasing cargo size. Extension of the cargo/C-peptide linker partially restores inhibitory potency. These results demonstrate that the human immunodeficiency virus defends its critical hairpin-forming machinery by steric exclusion of large proteins and may explain the current dearth of neutralizing Abs against the N-trimer. In contrast, previous results suggest the C-peptide region is freely accessible during fusion, demonstrating that the N- and C-peptide regions are in structurally distinct environments. Based on these results, we also propose new strategies for the generation of neutralizing Abs that overcome this steric block.

Human immunodeficiency virus (HIV)[1] entry is mediated by the viral envelope (Env) glycoprotein. Env is initially produced as gp160, which is proteolytically cleaved into non-covalently associated transmembrane (gp41) and surface (gp120) subunits. gp120 is primarily involved in recognition of cellular receptors, whereas gp41 is anchored in the viral membrane and mediates membrane fusion. The gp41 ectodomain contains two helical heptad repeat sequences (N- and C-peptide regions) (1, 2). Peptides corresponding to these helical regions (N- and C-peptides) are dominant-negative inhibitors of HIV membrane fusion (2, 3). Isolated N- and C-peptides form a six-helix bundle (trimer-of-hairpins) when mixed in solution (4–6). In this structure, three N-peptides form a central parallel trimeric coiled coil (N-trimer) surrounded by three anti-parallel C-peptides that nestle between neighboring N-peptides.

Based largely on these inhibitory and structural data, a working model of HIV-1 membrane fusion has been proposed (Fig. 1) (3, 5). Initial interaction of Env with its target cell occurs via gp120 binding to CD4 and a coreceptor (typically CCR5 or CXCR4). This binding induces a series of large conformational changes in gp120 that are propagated to gp41 via the gp41-gp120 interface. At this stage, gp41 transiently adopts an extended "prehairpin intermediate" conformation that bridges both the viral and cellular membranes. This state is believed to persist for at least 15 min (3, 7, 8) but eventually collapses into a trimer-of-hairpins structure that pulls both membranes into tight apposition and induces membrane fusion (Fig. 1).

In this model, the prehairpin intermediate exposes the isolated N-trimer, whereas the C-peptide region exists in an unknown and possibly unstructured conformation remote from the N-trimer (3). At this stage, the prehairpin intermediate is vulnerable to binding of exogenous N- and C-peptides. Binding of these peptide inhibitors denies access of the endogenous N- or C-peptide regions to their appropriate intramolecular partners, thwarting hairpin formation and membrane fusion. This model predicts that any molecule that binds to the prehairpin intermediate and disrupts association of the N- and C-peptides will inhibit membrane fusion and has been successfully applied to the development of several potent entry inhibitors (9–11).

Additionally, the gp41 prehairpin intermediate has several promising features as an inhibitory target (12). Peptide mimics of the N-trimer region have been structurally characterized at high resolution (4–6). The interface between the N- and C-peptides is highly conserved among diverse HIV strains of both laboratory-adapted and clinical isolates (9). The N-trimer also presents a long (>100 Å) deep groove with an extensive binding surface (4–6). These special properties have led many groups to search for Abs that can disrupt this interface (reviewed in Ref. 13).

C-peptide Inhibitors—Several peptide fusion inhibitors derived from the N- and C-peptide regions of gp41 have been described (2, 3, 12, 14–16). The most potent are peptides derived from the C-peptide region (*e.g.* C34, DP178/T20, T1249), which have low nM IC_{50}s against viral entry in cell-cell fusion (syncytia formation), and viral infectivity assays (reviewed in Ref. 17). Several mutations leading to T-20 resistance have been mapped to the N-peptide region of gp41 (18), providing strong support that the N-trimer is the primary target of C-peptide inhibitors.

* This work was supported in part by National Institutes of Health Grant P01GM066521 (to M. S. K.) and a National Institutes of Health training grant in biological chemistry (to B. D. W.). The costs of publication of this article were defrayed in part by the payment of page charges. This article must therefore be hereby marked "*advertisement*" in accordance with 18 U.S.C. Section 1734 solely to indicate this fact.

§ These authors contributed equally to this work.
¶ Present address: Dept. of Biology, 114-96, California Institute of Technology, Pasadena, CA 91125.
** To whom correspondence should be addressed: Dept. of Biochemistry, MREB 211, 50 N. Medical Dr., Salt Lake City, UT 84132. Tel.: 801-585-5021; Fax: 801-581-7959; E-mail: kay@biochem.utah.edu.

[1] The abbreviations used are: HIV, human immunodeficiency virus; Ab, antibody; Env, viral envelope glycoprotein; BPTI, bovine pancreatic trypsin inhibitor; Ub, human ubiquitin; Mb, sperm whale myoglobin; GFP, green fluorescent protein; MBP, maltose-binding protein; SPR, surface plasmon resonance.

gp41 N-trimer as a Vaccine Target—As demonstrated by the efficacy of C-peptide inhibitors, the N-trimer region of gp41 is a very attractive candidate for vaccine efforts. Many such efforts have been undertaken using various peptide mimics of the N-trimer region (*e.g.* N-peptide, 5-helix, IZN36, and $N35_{CCG}$-N13) (17, 19–21). These efforts have produced a large number of Abs with specific and high affinity binding to their targets but weak and/or narrow neutralizing activity in standard viral entry and spread assays. Interestingly, some of these anti-N-trimer Abs can inhibit fusion if bound to a temperature-arrested intermediate fusion state (19) or in the presence of soluble CD4 (21). Currently, there are only two reported anti-gp41 Abs that exhibit potent and broadly neutralizing activity, 2F5 and 4E10, which bind just outside the C-terminal border of the C-peptide region, an area with uncertain structure (reviewed in Ref. 22).

In this study, we tested the hypothesis that the N-trimer of gp41 is sterically restricted in the prehairpin intermediate, which may explain the current dearth of broadly neutralizing Abs against this target (Fig. 1). All of the known fusion inhibitors that target this structure (*e.g.* C34, T-20, T-1249, D-peptides) are small (<40 residue) peptides and could circumvent such a steric block. We have constructed fusions of a well characterized C-peptide inhibitor (C34) to a series of protein cargoes of varying sizes to determine whether such a steric block exists and, if so, to define its size cutoff. Our results demonstrate that C-peptide fusion proteins lose inhibitory potency with increasing size and that the N-trimer region of gp41 is likely to be poorly accessible to proteins as large as Abs. These results have important implications for gp41 vaccine design as well as for the production of second-generation C-peptide entry inhibitors. This steric restriction also helps to better define the conformation of the prehairpin intermediate.

MATERIALS AND METHODS

Reagents—Plasmids were obtained from the following sources: pET vectors (Novagen), pMAL-c2G (New England Biolabs), pEBB-HXB2 and pEBB-JRFL (gifts from B. Chen) (23). Reverse phase HPLC was performed using a C18 column (Vydac). All Ni affinity purifications used His-Select HC nickel affinity gel (Sigma) or His-Select HC nickel magnetic resin (Sigma). The National Institutes of Health AIDS Research and Reference Reagent Program provided the following reagents: pNL4–3.Luc.R-E- (N. Landau), HeLa-CD4-LTR-β-galactosidase cells (M. Emerman), HOS-CD4-fusin/CCR5 cells (N. Landau).

Protein Expression, Purification, and Characterization—C37-H6 (C37), derived from the HXB2 Env sequence, was expressed and purified as previously described (9). Proteins used in this study were bovine pancreatic trypsin inhibitor (BPTI), human ubiquitin (Ub), sperm whale myoglobin (Mb), enhanced green fluorescent protein (GFP; Clontech), and *Escherichia coli* maltose-binding protein (MBP; New England Biolabs). Linker sequences were Ser_4Gly_2 for BPTI-C37, Ub-C37, and GFP-C37 and Ser_5Gly_2 for Mb-C37 and MBP-C37 (linker sequences are slightly different for cloning reasons). The extended linker constructs had the following linker sequences: $SSS(GGGS)_3$-SSSGG (MBP1-C37) and $SSS(GGGS)_3S(GGGS)_3$SSSGG (MBP2-C37). The DNA encoding each protein was cloned into the following plasmids: pET9a (for BPTI-C37, Ub-C37, Mb-C37, and GFP-C37), pET20b (for BPTI-H6, Ub-H6, Mb-H6, and GFP-H6); pMAL-c2G (for MBP-H6, MBP-C37, MBP1-C37, and MBP2-C37). Proteins were expressed in BL21(DE3)pLysS (Novagen) for pET9a and pET20b vectors and XL1-Blue (Stratagene) for pMal-c2G vectors. All proteins have C-terminal His tags (His_6) and were purified using Ni affinity chromatography.

BPTI required refolding after expression for correct formation of disulfide bonds. Briefly, after Ni affinity purification, BPTI-C37-H6 and BPTI-H6 were reduced with 100 mM β-mercaptoethanol at pH 8 and dialyzed into 5% acetic acid. The proteins were air oxidized in the presence of a 1:10 ratio of oxidized:reduced glutathione at pH 8, 4 °C for 24 h. The correctly folded proteins were isolated using reverse phase HPLC and were confirmed by near-UV circular dichroism (Aviv 62DS) and measurement of trypsin inhibiting activity as previously described (24).

Cys-Gly-Gly-Asp-IZN36 (10) was cloned into pET14b and expressed in BL21(DE3)pLysS. IZN36 was purified from inclusion bodies (solubilized in 6 M GuHCl) using Ni affinity chromatography. The protein was then dialyzed into 5% acetic acid and purified by reverse phase HPLC. This material was reduced with TCEP (Pierce) and biotinylated at its unique Cys residue using Biotin-HPDP (Pierce). After biotinylation, the His tag was removed by thrombin cleavage (Novagen), and the cleaved product was purified by reverse phase HPLC. The sequence of the final product is GSHMCGGDIKKEIEAIKKEQEAIKKKIEAIEKEISGIVQQQNNLLRAIEAQQHLLQLTVWGIKQLQARIL.

All protein masses were confirmed by matrix-assisted laser desorption ionization or electrospray mass spectrometry (University of Utah Core Facility). All proteins were judged >98% pure by SDS-PAGE. Protein concentrations were measured by UV absorbance at 280 nm (25).

Surface Plasmon Resonance (SPR) Analysis—Binding experiments were performed using a Biacore 2000 optical biosensor (University of Utah Protein Interaction Core Facility) equipped with research-grade CM5 sensor chips (Biacore). A standard coupling protocol was employed to immobilize streptavidin (SA; Pierce) (26). Biotinylated IZN36 was captured on a SA surface, and free SA surfaces served as references.

Binding analysis of C37 and C37 fusion proteins was performed at 25 °C with a data collection rate of 2.5 Hz. The binding buffer (phosphate-buffered saline; Invitrogen) + 0.005% P20 detergent (Biacore) + 1 mg/ml bovine serum albumin (fraction V; Fisher)) was prepared, vacuum filtered, and degassed immediately prior to use. Stock solutions of C37, C37 fusion proteins, and corresponding control proteins (without C37) were prepared in binding buffer at 100 nM. Protein binding was analyzed by injecting samples for 1 min over the IZN36 and reference surfaces using KINJECT at a flow rate of 50–100 μl/min. The dissociations were monitored for 3 min. The IZN36 surfaces were completely regenerated using one 3-s pulse of 6 M guanidine-HCl or three 6-s pulses of 0.1% SDS.

Data from the reference flow cells were subtracted to remove systematic artifacts that occurred in all flow cells (27). The data were normalized to the highest point in the response curve to facilitate comparison. Binding at one concentration was analyzed using a 1:1 binding model in CLAMP (28), assuming enough information from the curvature of the responses to determine the approximate kinetic parameters for the reactions (29).

Cell-cell Fusion and Viral Infectivity Assay—Cell-cell fusion was monitored as previously described (30). Briefly, HXB2 Env-expressing Chinese hamster ovary cells (gift from M. Krieger (31)) were mixed with HeLa-CD4-LTR-β-galactosidase cells in the presence of inhibitors for 20 h at 37 °C. Syncytia were stained with 5-bromo-4-chloro-3-indolyl-β-D-galactopyranoside (X-gal) (Invitrogen) and counted.

Viral infectivity was measured as previously described (9). Briefly, pseudotyped viruses were produced by co-transfecting 293T cells using FuGENE (Roche Applied Science) with pNL4–3.Luc.R-E- and either pEBB-HXB2 or pEBB-JRFL. After 36–48 h, viral supernatants were collected and sterile filtered. HXB2 or JRFL pseudotyped virus was added to HOS-CD4-fusin or HOS-CD4-CCR5 cells, respectively, in the presence of inhibitors. HXB2 assays included 20 μg/ml DEAE-dextran (23). After 12 h, virus and inhibitor were removed and replaced with fresh media. Cells were lysed 40–44 h after infection using Glo lysis buffer (Promega), and luciferase activity was measured using Bright-Glo (Promega). IC_{50} values for both assays were calculated by fitting data to the equation, $y = k/(1 + [\text{inhibitor}]/IC_{50})$, where y is the normalized number of syncytia or luciferase activity and k is the scaling constant ($k = 1$ for syncytia assay and is floated for viral infectivity assay, see Fig. 2*B* legend).

Assays for Inhibitor Proteolysis and Precipitation—C37 fusion inhibitors were incubated in tissue culture medium (Dulbecco's modified Eagle's medium + 10% fetal bovine serum; Invitrogen) at 37 °C for 20 h. Proteins were purified from the medium by a 1-h incubation at room temperature with magnetic Ni affinity beads. The resin was washed 3× with phosphate-buffered saline, and proteins were eluted by boiling in LDS sample buffer (Invitrogen). Eluted samples were separated by SDS-PAGE and visualized with SimplyBlue stain (Invitrogen). Unpurified media samples were analyzed before and after centrifugation (10 min. at 18,000 × *g*) by Western blot using polyclonal rabbit anti-His tag Ab (Abcam) and SuperSignal West Pico substrate (Pierce), as well as visually analyzed for precipitate.

RESULTS

Production of Fusion Proteins—To test for steric constraints in accessing the gp41 N-trimer region, we constructed a series of inhibitors containing a C-peptide attached to cargo proteins

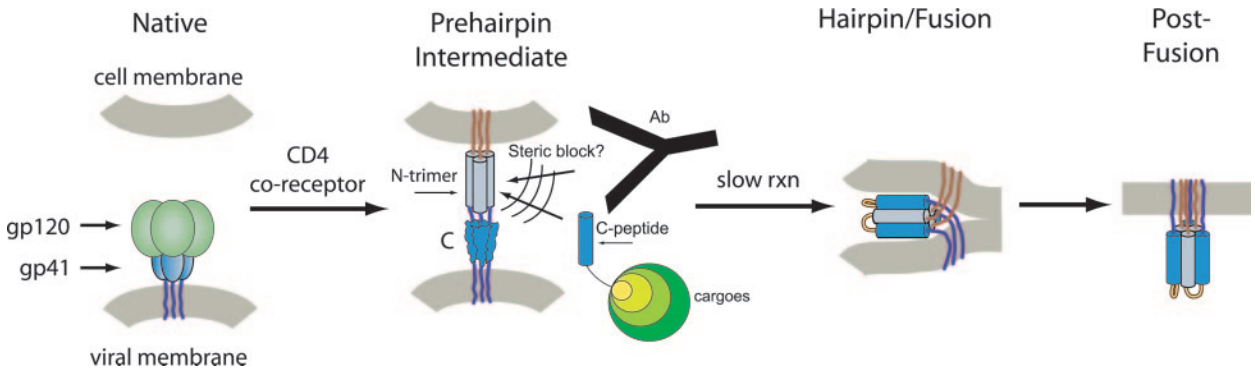

FIG. 1. **Model of HIV-1 membrane fusion pathway (adapted from Ref. 9).** Formation of the trimer-of-hairpins drives the viral and cellular membranes together, leading to fusion. The N-peptide region (*gray*), C-peptide region (*blue*), gp120 (*green*), gp41 (*light blue*), gp41 fusion peptide (*red*), and transmembrane domain (*purple*) are shown. gp120 is removed from the prehairpin intermediate for clarity. Also shown are a series of C37 fusion proteins of different sizes and an anti-N-trimer Ab attempting to access the N-trimer but potentially blocked by a steric restriction. Sizes of the Ab and fusion proteins are only approximately to scale.

of various sizes (Fig. 1). The cargo partners used in this study were selected for the following properties: monomeric, soluble, globular, stable, tolerant to C-terminal additions, and free of nonspecific peptide binding. Cargo proteins meeting these inclusion criteria and used in this study range from 6 to 41 kDa (Table I). For these studies, C37 (9), the recombinant His-tagged version of the previously characterized synthetic peptide C34 (30, 32), was used as the reference inhibitor. In each fusion protein, C37 is connected at its N terminus to the C terminus of the cargo by a flexible 6- or 7-residue Ser/Gly linker. This linker was designed to be long enough to allow the proper orientation of C37 as it binds to the N-trimer but short enough for the attached cargo to prevent access to an occluded binding site. The N terminus of C37 was chosen for attachment of cargo because this attachment site points away from the membrane (whereas the C terminus of C37 is expected to be near the viral membrane and, therefore, less accessible; see Fig. 1). For each fusion protein, a matching control protein lacking C37 was also produced.

Size and Inhibitory Potency Are Inversely Correlated—The inhibitory potency of each inhibitor was tested using a cell-cell fusion (syncytia) assay utilizing HXB2 Env and two viral infectivity assays utilizing either HXB2 (X4) or JRFL (R5) Envs (Table I, Fig. 2). C37 shows high potency inhibition in all assays (IC_{50} = 0.85–8.2 nM). Inhibition is slightly weaker than seen with C34 (30), as expected from the loss of helix-stabilizing synthetic blocking groups found in C34. For reference, the anti-gp41 Abs 2F5 and 4E10 have reported IC_{50} values of ~0.2–7 nM against HXB2/IIIB laboratory strains in cell-cell and viral infectivity assays similar to those used in this study (33, 34).

The smallest fusion protein, BPTI-C37, also displays high potency in both assays, very similar to C37, demonstrating that our C37-cargo linker does not interfere with inhibitory activity. Ub-C37 is a slightly weaker (2.5–5.5-fold) inhibitor than C37, whereas Mb-C37 and GFP-C37 both show more substantial (21–65-fold) reductions in potency in both assays. MBP-C37 shows the most dramatic change with a 75–228-fold drop in potency. None of the control proteins (cargo without C37 peptide) inhibits at up to 1 μM (10 μM for MBP with JRFL Env) in either assay (data not shown).

In general, the cell-cell fusion and viral infectivity assays show similar losses of activity with increasing size of the inhibitors, with a slightly more pronounced effect on cell-cell fusion and JRFL-mediated viral entry. For HXB2 Env we observed up to a 4-fold greater potency in cell-cell fusion *versus* viral infectivity as seen in studies of other fusion inhibitors (2, 11, 30, 35). As expected, inhibitors were less potent against the primary isolate JRFL in the viral infectivity assay. For most of the inhibitors, the viral infectivity data show a reproducible increase in infectivity (above the uninhibited values) at low inhibitor concentrations (see the legend to Fig. 2*B*). This "overshoot" has also occasionally been seen in other studies of fusion inhibitors (36–38) but has not been explained.

The C-peptide Remains Accessible when Linked to Fusion Partners—To ensure that linkage of C37-H6 to each of the partner proteins did not affect the accessibility of C37 for binding to a sterically open target, the fusion proteins and C37 were assayed for binding to IZN36, a soluble mimic of the N-trimer (10), using SPR. Each fusion protein was flowed over the control and IZN36 surfaces. C37 reversibly bound to IZN36 with a low nM K_D (Fig. 3). The calculated K_D for the fusion proteins are clustered in a narrow range around the C37 value (2-fold lower to 2-fold higher). The estimated kinetic parameters are similarly clustered, ranging from 3.2-fold slower to 1.4-fold faster (association rate) and up to 3.2-fold slower (dissociation rate). These rates are only approximate due to small systematic deviations from the fitting model, but as expected there is a slight trend toward slower association and dissociation rates with increasing molecular weight. These small differences in binding kinetics are likely responsible for some of the variation in potency observed here but rule out distinct binding kinetics as the major contributor to the substantial differences in potency among these inhibitors. These results also show that the accessibility and affinity of C37 are not significantly altered in the context of the fusion proteins. None of the cargo proteins alone showed measurable association with IZN36 at 100 nM (Fig. 3, *inset*).

Partial Restoration of Inhibitory Potency with Extended Gly/Ser Linkers—To test whether a longer linker could overcome the steric block and restore inhibitory potency of our weakest inhibitor, we extended the flexible linker in MBP-C37 from its original length of 7 amino acids to 20 (MBP1-C37) or 33 (MBP2-C37) using Gly/Ser residues (Table I). Both extended linker inhibitors exhibit partial recovery of inhibitory potency. Compared with MBP-C37, MBP1-C37 and MBP2-C37 are 2.3–2.9-fold and 2.6–6.1-fold more potent, respectively (Table I). Compared with MBP-C37, MBP1- and MBP2-C37 interact similarly with IZN36 as measured by SPR (K_D vary by <20%, k_a and k_d are <2-fold higher). In contrast to the other cargo-C37 fusions, a significant portion of the increased potency in MBP1- and MBP2-C37 may be attributable to an increased association rate.

Stability of Fusion Proteins during Fusion Assays—Inhibitors were analyzed for precipitation or extensive proteolysis to demonstrate that these processes did not cause the observed decrease in potency of the fusion proteins. C37 and the C37

TABLE I
IC_{50} (in nM) of fusion proteins in cell-cell fusion and viral infectivity assays

Protein	Fusion partner molecular mass	Cell-cell fusion	IC_{50} ratio (cell-cell fusion)	Viral infectivity HXB2	IC_{50} ratio HXB2	Viral infectivity JRFL	IC_{50} ratio JRFL
	kDa						
C37	0	0.85	1.0	2.8	1.0	8.2	1.0
BPTI-C37	6.5	1.5	1.8	3.1	1.1	4.8	0.6
Ub-C37	8.6	4.7	5.5	6.8	2.5	37.7	4.6
Mb-C37	17	30.8	36.2	58.0	21.0	414	50.5
GFP-C37	27	28.9	34.0	118	42.8	533	65.0
MBP-C37	41	192	225	206	74.8	1874	228
MBP1-C37	41	75.1	88.4	88.9	32.2	640	78.0
MBP2-C37	41	31.2	36.7	79.2	28.7	516	62.9

IC_{50} S.E. is <25% for both assays. IC_{50} ratios are relative to C37.

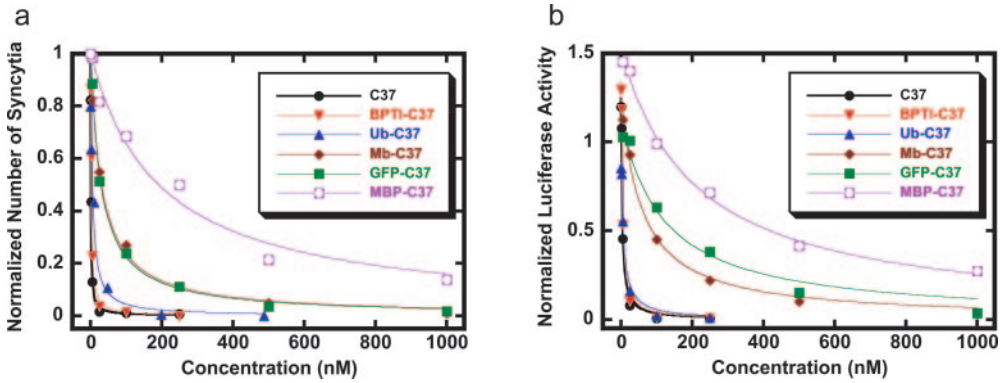

FIG. 2. **Inhibitory activity of C37 and C37 fusion proteins.** Data points are averages of at least quadruplicate measurements. Data are normalized to uninhibited fusion activity. *a*, cell-cell fusion assay (HXB2 Env). S.E. of each point is <0.05. *b*, viral infectivity assay (HXB2 Env). S.E. of each point is <0.1. An overshoot is observed at low inhibitor concentrations (data above 1.0). Fitting the viral infectivity data to a simple Langmuir equation with a fixed zero inhibitor point produces noticeable deviation from the data near the zero point because of this overshoot. Fitting the data without fixing the zero inhibitor point (as done in this study) improves the quality of the fit but does not significantly affect the relative IC_{50} values of the inhibitors.

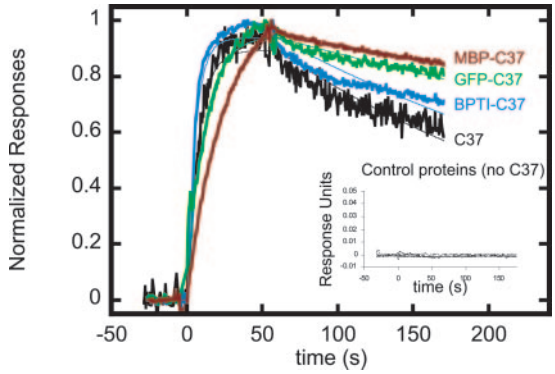

FIG. 3. **Binding of C37 and C37 fusion inhibitors to IZN36 measured by SPR.** Responses for representative inhibitors were normalized and overlaid to facilitate their comparison (*thick traces*). Fits to the interaction model are included (*thin traces*). *Inset*, interaction of control proteins (no C37) with IZN36 surface.

fusions were incubated in tissue culture medium at 37 °C for 20 h to simulate the harshest conditions faced by the inhibitors during the cell-cell fusion and viral infectivity assays. We observed only trace (<2%) degradation for all of the inhibitors (data not shown), allowing us to conclude that proteolysis did not cause a significant decrease in the potency of our inhibitors. We cannot, however, rule out the contribution of minor proteolytic breakdown products to increased inhibitory potency, particularly for the least potent inhibitors (1% contamination with free C37 would result in an apparent cell-cell fusion IC_{50} value of ~100 nM for a completely inactive inhibitor). Therefore, the described potencies of the inhibitors presented in this study should be considered an upper limit. An anti-His tag Western blot comparing samples before and after high speed centrifugation revealed no precipitation (data not shown).

DISCUSSION

In principle, the gp41 N-trimer is an especially promising inhibition target, but despite the generation of numerous Abs with tight and specific binding against various mimics of the N-trimer, none of these Abs displays broadly neutralizing activity (reviewed in Ref. 17). Our results suggest that HIV may have developed a strong steric defense against immune attack for its critical N-trimer region. In this study we have shown that the gp41 N-trimer region has poor accessibility to large proteins. It is a logical extrapolation of the data presented here that a protein as large as IgG (150 kDa), even though it forms a somewhat elongated shape, will suffer a steric block at least as severe as we observed with our largest protein, MBP (41 kDa), which is smaller than the individual (~50 kDa) domains of an IgG. This defense may be a major factor in frustrating efforts to induce neutralizing Abs against the N-trimer region and may also explain why such neutralizing Abs against the N-trimer have not yet been observed in infected patients.

The steric restriction of the N-trimer stands in stark contrast to apparent accessibility of the extreme C-terminal region of the gp41 ectodomain (between the C-peptide region and the transmembrane domain). The only known potent and broadly neutralizing Abs against gp41 (2F5 and 4E10) target this region (22). Recent studies have suggested that this region may adopt a helical or β-strand conformation or cycle between the two (33, 39). For the most thoroughly studied Ab against this region, 2F5, a full-length IgG (~150 kDa), is more potent than the Fab (~50 kDa) (33), suggesting a freely accessible site.

There is also evidence suggesting that the C-peptide region may be more accessible than the N-trimer. The designed proteins 5-helix (25 kDa) (9) and N_{CCG}-gp41 (35 kDa) (40) target the C-peptide region and are potent entry inhibitors. Recently, a *Pseudomonas* endotoxin (PE) fusion with 5-helix (5-helix-PE,

65 kDa) was shown to inhibit viral entry with similar potency as 5-helix (41), although a toxic effect from PE may mask a loss of potency. Although the C-peptide region is likely accessible, it is difficult to target for vaccine studies, as it is unclear what organized structure (if any) this region adopts during viral entry.

C37 inhibits viral fusion by binding along the full length of the surface groove of the N-trimer, including the deep hydrophobic "pocket" region previously shown to be an essential player in viral fusion. Inhibitors that specifically target this pocket have been developed (10).[2] In future studies, it will be important to test such pocket-specific inhibitors to see whether they can circumvent the steric block observed here. It will also be important to check whether cargo fused to the C terminus of C37 shows a similar pattern of steric blockage.

The steric block we observe in the gp41 N-trimer is reminiscent of steric restrictions observed in gp120. These restrictions have been attributed to glycosylation ("glycan shield") (42, 43) and/or inaccessible antigens (38, 44, 45). Previous studies with several broadly neutralizing gp120 Abs have shown that smaller versions of these Abs (Fabs or scFvs) often have significantly improved potency despite a loss of avidity (38, 46). The N-trimer steric block observed here may be more strict than seen in gp120. Proteins the size of Fabs (~50 kDa) and scFvs (~25 kDa) are already too large to fully access the gp41 N-trimer. Interestingly, the N-trimer region does not contain any glycosylation sites, probably because of its ultimate complete burial in the six-helix bundle structure. The N-trimer, however, may be affected by nearby glycosylation sites in gp120 or other regions of gp41 (the C-peptide region and N/C-peptide connecting loop are extensively glycosylated). A glycosylation site near the gp120 V3 loop has been shown to affect accessibility of the 2F5 Ab to its gp41 epitope in resistant strains (43).

Implications for C-peptide Inhibitors—Our results suggest that attempts to improve the longevity of C-peptide inhibitors in the bloodstream may also be frustrated by steric issues. For instance, T-20, a 36-residue peptide recently approved by the FDA, is rapidly cleared from the bloodstream by kidney filtration, dramatically increasing dosing requirements. A reasonable approach for prevention of this rapid clearance is to cross-link C-peptide inhibitors to larger proteins (*e.g.* albumin) or high molecular weight polyethylene glycol, which also can reduce peptide immunogenicity (47). Our results suggest that these straightforward approaches will likely reduce the potency of modified C-peptides, although use of smaller proteins or low molecular weight polyethylene glycol may lessen this effect. Our extended loop constructs suggest the possibility that longer linkers between these bulking groups and the C-peptide inhibitor could improve accessibility to the N-trimer. Stiffer (*e.g.* helical) linkers may provide better separation from large fusion partners and restore inhibitory potency better than the flexible Gly/Ser linkers employed here.

An important caveat to applying our results to T-20 is that, compared with C34, T-20 is derived from a gp41 sequence shifted about 10 amino acids toward the C terminus and its binding site extends beyond the N-trimer region. Although they are thought to have a similar mechanism of action, T-20 and C34 (and the similar T-1249) vary in their potencies against different HIV-1 strains and their sensitivities to resistance mutations (18, 48, 49).

Future Directions: Overcoming the Steric Block—We hope that the observation of this steric block can be used to improve the chances of discovering a broadly neutralizing Ab against this valuable HIV target, rather than discouraging this effort. Specifically, we suggest that a designed, sterically restricted N-trimer antigen could be used to generate, boost, or screen for potent neutralizing Abs able to overcome the steric block. Currently used mimics of the N-trimer region (*e.g.* 5-helix, IZN36, N_{CCG}-gp41) could be modified by attachment to bulky proteins or large inert particles such that only Abs capable of penetrating a sterically recessed target would be selected.

Neutralizing Abs against sterically blocked gp120 targets often utilize unusually long CDR H3 loops to access recessed antigens (33, 46, 50). The insertion of longer linkers connecting MBP to C37 results in partial recovery of inhibitory activity, suggesting that extended CDR H3 loops may help penetrate the steric block on the gp41 N-trimer. These Abs are difficult to generate in small animals, as Abs in primates have longer CDR H3 loops on average than rodents (51). Potent N-trimer Abs may be more easily found using strategies that enrich for this type of Ab (*e.g.* engineered Ab libraries, Ab phage display, immunization of primates). Alternatively, very high affinity (sub-nM) Abs against the N-trimer may still be sufficiently neutralizing despite a substantial decrease in potency caused by the steric block. Recently, Merck has reported preliminary results on an antibody that binds to the N-trimer region and possesses neutralizing activity against some HIV strains (52). No detailed information on this Ab has yet been published, but it will be interesting to see whether or how this Ab circumvents the steric block we observe here (*e.g.* high affinity Ab that can tolerate several hundred-fold loss in activity, extended variable loops, specific targeting of a subsite in the N-trimer).

Finally, our results suggest that the traditional depiction of the prehairpin intermediate as a symmetric structure (*e.g.* Fig. 1) may be inaccurate. The steric block of the N-trimer and apparent accessibility of the C-peptide region show that they reside in very different environments. Possible sources of this asymmetry include interactions with gp120, other regions of gp41, or cell surface proteins as well as glycosylation and differences between the curvature of the viral and cellular membranes.

Acknowledgments—We thank Peter Kim, in whose laboratory this work originated. We also thank D. Goldenberg (BPTI folding), D. Myszka and the Protein Interaction Group at the University of Utah (SPR), N. Welker, B. Stadtmueller, B. Kelly, C. Kieffer, and K. Rigby (protein production), W. Sundquist and C. Hill (advice and support), U. von Schwedler, B. Chen, V. Planelles, and M. Root (virology advice and assistance), and D. Eckert (invaluable discussions and critical review of the manuscript).

REFERENCES

1. Lu, M., Blacklow, S. C., and Kim, P. S. (1995) *Nat. Struct. Biol.* **2,** 1075–1082
2. Wild, C. T., Shugars, D. C., Greenwell, T. K., McDanal, C. B., and Matthews, T. J. (1994) *Proc. Natl. Acad. Sci. U. S. A.* **91,** 9770–9774
3. Chan, D. C., and Kim, P. S. (1998) *Cell* **93,** 681–684
4. Tan, K., Liu, J., Wang, J., Shen, S., and Lu, M. (1997) *Proc. Natl. Acad. Sci. U. S. A.* **94,** 12303–12308
5. Weissenhorn, W., Dessen, A., Harrison, S. C., Skehel, J. J., and Wiley, D. C. (1997) *Nature* **387,** 426–430
6. Chan, D. C., Fass, D., Berger, J. M., and Kim, P. S. (1997) *Cell* **89,** 263–273
7. Munoz-Barroso, I., Durell, S., Sakaguchi, K., Appella, E., and Blumenthal, R. (1998) *J. Cell Biol.* **140,** 315–323
8. Melikyan, G. B., Markosyan, R. M., Hemmati, H., Delmedico, M. K., Lambert, D. M., and Cohen, F. S. (2000) *J. Cell Biol.* **151,** 413–423
9. Root, M. J., Kay, M. S., and Kim, P. S. (2001) *Science* **291,** 884–888
10. Eckert, D. M., and Kim, P. S. (2001) *Proc. Natl. Acad. Sci. U. S. A.* **98,** 11187–11192
11. Eckert, D. M., Malashkevich, V. N., Hong, L. H., Carr, P. A., and Kim, P. S. (1999) *Cell* **99,** 103–115
12. Eckert, D. M., and Kim, P. S. (2001) *Annu. Rev. Biochem.* **70,** 777–810
13. Burton, D. R., Desrosiers, R. C., Doms, R. W., Koff, W. C., Kwong, P. D., Moore, J. P., Nabel, G. J., Sodroski, J., Wilson, I. A., and Wyatt, R. T. (2004) *Nat. Immunol.* **5,** 233–236
14. Wild, C., Oas, T., McDanal, C., Bolognesi, D., and Matthews, T. (1992) *Proc. Natl. Acad. Sci. U. S. A.* **89,** 10537–10541
15. Wild, C., Greenwell, T., and Matthews, T. (1993) *AIDS Res. Hum. Retroviruses* **9,** 1051–1053
16. Jiang, S., Lin, K., Strick, N., and Neurath, A. R. (1993) *Nature* **365,** 113
17. Weiss, C. D. (2003) *AIDS Rev.* **5,** 214–221
18. Rimsky, L. T., Shugars, D. C., and Matthews, T. J. (1998) *J. Virol.* **72,** 986–993

[2] B. D. Welch and M. S. Kay, unpublished results.

19. Golding, H., Zaitseva, M., de Rosny, E., King, L. R., Manischewitz, J., Sidorov, I., Gorny, M. K., Zolla-Pazner, S., Dimitrov, D. S., and Weiss, C. D. (2002) *J. Virol.* **76,** 6780–6790
20. Opalka, D., Pessi, A., Bianchi, E., Ciliberto, G., Schleif, W., McElhaugh, M., Danzeisen, R., Geleziunas, R., Miller, M., Eckert, D. M., Bramhill, D., Joyce, J., Cook, J., Magilton, W., Shiver, J., Emini, E., and Esser, M. T. (2004) *J. Immunol. Methods* **287,** 49–65
21. Louis, J. M., Nesheiwat, I., Chang, L., Clore, G. M., and Bewley, C. A. (2003) *J. Biol. Chem.* **278,** 20278–20285
22. McGaughey, G. B., Barbato, G., Bianchi, E., Freidinger, R. M., Garsky, V. M., Hurni, W. M., Joyce, J. G., Liang, X., Miller, M. D., Pessi, A., Shiver, J. W., and Bogusky, M. J. (2004) *Curr. HIV Res.* **2,** 193–204
23. Chen, B. K., Saksela, K., Andino, R., and Baltimore, D. (1994) *J. Virol.* **68,** 654–660
24. Coplen, L. J., Frieden, R. W., and Goldenberg, D. P. (1990) *Proteins* **7,** 16–31
25. Edelhoch, H. (1967) *Biochemistry* **6,** 1948–1954
26. Johnsson, B., Lofas, S., and Lindquist, G. (1991) *Anal. Biochem.* **198,** 268–277
27. Myszka, D. G. (1999) *J. Mol. Recognit.* **12,** 279–284
28. Myszka, D. G., and Morton, T. A. (1998) *Trends Biochem. Sci.* **23,** 149–150
29. Canziani, G. A., Klakamp, S., and Myszka, D. G. (2004) *Anal. Biochem.* **325,** 301–307
30. Chan, D. C., Chutkowski, C. T., and Kim, P. S. (1998) *Proc. Natl. Acad. Sci. U. S. A.* **95,** 15613–15617
31. Kozarsky, K., Penman, M., Basiripour, L., Haseltine, W., Sodroski, J., and Krieger, M. (1989) *J. Acquir. Immune Defic. Syndr.* **2,** 163–169
32. Malashkevich, V. N., Chan, D. C., Chutkowski, C. T., and Kim, P. S. (1998) *Proc. Natl. Acad. Sci. U. S. A.* **95,** 9134–9139
33. Zwick, M. B., Komori, H. K., Stanfield, R. L., Church, S., Wang, M., Parren, P. W., Kunert, R., Katinger, H., Wilson, I. A., and Burton, D. R. (2004) *J. Virol.* **78,** 3155–3161
34. Stiegler, G., Kunert, R., Purtscher, M., Wolbank, S., Voglauer, R., Steindl, F., and Katinger, H. (2001) *AIDS Res. Hum. Retroviruses* **17,** 1757–1765
35. Sia, S. K., and Kim, P. S. (2003) *Proc. Natl. Acad. Sci. U. S. A.* **100,** 9756–9761
36. Wei, X., Decker, J. M., Liu, H., Zhang, Z., Arani, R. B., Kilby, J. M., Saag, M. S., Wu, X., Shaw, G. M., and Kappes, J. C. (2002) *Antimicrob. Agents Chemother.* **46,** 1896–1905
37. Reeves, J. D., Gallo, S. A., Ahmad, N., Miamidian, J. L., Harvey, P. E., Sharron, M., Pohlmann, S., Sfakianos, J. N., Derdeyn, C. A., Blumenthal, R., Hunter, E., and Doms, R. W. (2002) *Proc. Natl. Acad. Sci. U. S. A.* **99,** 16249–16254
38. Labrijn, A. F., Poignard, P., Raja, A., Zwick, M. B., Delgado, K., Franti, M., Binley, J., Vivona, V., Grundner, C., Huang, C. C., Venturi, M., Petropoulos, C. J., Wrin, T., Dimitrov, D. S., Robinson, J., Kwong, P. D., Wyatt, R. T., Sodroski, J., and Burton, D. R. (2003) *J. Virol.* **77,** 10557–10565
39. Barbato, G., Bianchi, E., Ingallinella, P., Hurni, W. H., Miller, M. D., Ciliberto, G., Cortese, R., Bazzo, R., Shiver, J. W., and Pessi, A. (2003) *J. Mol. Biol.* **330,** 1101–1115
40. Louis, J. M., Bewley, C. A., and Clore, G. M. (2001) *J. Biol. Chem.* **276,** 29485–29489
41. Root, M. J., and Hamer, D. H. (2003) *Proc. Natl. Acad. Sci. U. S. A.* **100,** 5016–5021
42. Wei, X., Decker, J. M., Wang, S., Hui, H., Kappes, J. C., Wu, X., Salazar-Gonzalez, J. F., Salazar, M. G., Kilby, J. M., Saag, M. S., Komarova, N. L., Nowak, M. A., Hahn, B. H., Kwong, P. D., and Shaw, G. M. (2003) *Nature* **422,** 307–312
43. McCaffrey, R. A., Saunders, C., Hensel, M., and Stamatatos, L. (2004) *J. Virol.* **78,** 3279–3295
44. Kwong, P. D., Wyatt, R., Robinson, J., Sweet, R. W., Sodroski, J., and Hendrickson, W. A. (1998) *Nature* **393,** 648–659
45. Saphire, E. O., Parren, P. W., Pantophlet, R., Zwick, M. B., Morris, G. M., Rudd, P. M., Dwek, R. A., Stanfield, R. L., Burton, D. R., and Wilson, I. A. (2001) *Science* **293,** 1155–1159
46. Choe, H., Li, W., Wright, P. L., Vasilieva, N., Venturi, M., Huang, C. C., Grundner, C., Dorfman, T., Zwick, M. B., Wang, L., Rosenberg, E. S., Kwong, P. D., Burton, D. R., Robinson, J. E., Sodroski, J. G., and Farzan, M. (2003) *Cell* **114,** 161–170
47. Harris, J. M., and Chess, R. B. (2003) *Nat. Rev. Drug. Discov.* **2,** 214–221
48. Reeves, J. D., Miamidian, J. L., Biscone, M. J., Lee, F. H., Ahmad, N., Pierson, T. C., and Doms, R. W. (2004) *J. Virol.* **78,** 5476–5485
49. Kliger, Y., Gallo, S. A., Peisajovich, S. G., Munoz-Barroso, I., Avkin, S., Blumenthal, R., and Shai, Y. (2001) *J. Biol. Chem.* **276,** 1391–1397
50. Zwick, M. B., Parren, P. W., Saphire, E. O., Church, S., Wang, M., Scott, J. K., Dawson, P. E., Wilson, I. A., and Burton, D. R. (2003) *J. Virol.* **77,** 5863–5876
51. Wu, T. T., Johnson, G., and Kabat, E. A. (1993) *Proteins* **16,** 1–7
52. Miller, M., and Geleziunas, R. (2004) *Abstracts of the 13th International HIV Drug Resistance Workshop*, Tenerife Sur-Costa Adeje, Canary Islands, Spain, June 8–12, 2004 Abstract 9, International Medical Press, Ltd., London